Arabian Journal for Science and Engineering
https://doi.org/10.1007/s13369-024-08748-6

RESEARCH ARTICLE-CHEMISTRY

Decolorization of Congo Red and Reactive Black 5 Dyes with Horseradish Peroxidase-Immobilized Cross-Linked Polymeric Microbeads

Altynay Zhumabekova[1] · Samir Abbas Ali Noma[1] · Elif Tümay Özer[1] · Bilgen Osman[1]

Received: 1 October 2023 / Accepted: 11 January 2024

Abstract
In this study, the efficiency of poly(ethylene glycol dimethacrylate-*N*-methacryloyl-amido-L-tryptophan methyl ester) [PEDMT] microbeads (in the diameter range of 106–180 μm) as a support material for HRP immobilization was evaluated and the immobilized-HRP enzyme was used for decolorization of Congo Red (CR) and Reactive Black 5 (RB5) dyes. The specific surface area of the PEDMT microbeads was 1103 m^2 g^{-1}, which is very high. The PEDMT microbeads had a pore volume and pore size of 1.94 cm^3 g^{-1} and 9.99–55.3 Å, respectively. The chemical compositions of the PEDMT and PEDMT–HRP microbead surfaces were analyzed using X-ray photoelectron spectroscopy (XPS). Immobilization yield, activity yield, and immobilization efficiency were 84.9 ± 2.1, 73.8 ± 5.9%, and 86.9 ± 6.9%, respectively. Optimum pH (6.0), temperature (45 °C and 50 °C for free and immobilized enzyme), H_2O_2 concentration (3% *v/v*) were investigated in detail. Thermal and storage stability was increased after immobilization and immobilized enzyme preserved more than 55% of its initial activity even after 10 consecutive uses. Decolorization studies were also performed by investigating the effects of pH, CR, and RB5 concentration, enzyme amount, H_2O_2 concentration, contact time on decolorization efficiency. The decolorization efficiency for CR and RB5 by PEDMT–HRP was 98.20% and 47.99% after 30 min at pH 6.0 and 45 °C. The immobilized-HRP retained 89% and 27% of its initial activity after three repeated cycles with CR and RB5, respectively. The PEDMT microbeads with high surface area, porosity, durability, and reusability exactly met the requirements for HRP immobilization and dye decolorization.

Keywords Horseradish peroxidase · Immobilization · Decolorization · Congo Red · Reactive Black 5 · Polymeric microbeads

1 Introduction

Water pollution caused by the rapid increase in population and industrialization has been a big concern in the last century. One leading reason for water pollution is the discharge of large amounts of industrial waste contaminated with synthetic dyes into natural water reservoirs [1]. Around 90% of the azo dyes are assumed to be released into the environment without adequate treatment [2]. Azo dyes are toxic, carcinogenic, and non-biodegradable dyes which are widely used in various industries [3, 4]. They contribute about 70% of total dyes consumption [2], and they adversely affect the photosynthetic function of aquatic life, turning into harmful products when thrown into the environment [5]. They are known to be very durable and persistent due to their complicated structure; therefore, it is challenging to decolorize them by conventional biological processes. Different physicochemical decolorization methods have been investigated, such as coagulation, adsorption [6], ozonation, photocatalysis, membrane treatment, and precipitation. However, the expensiveness of these methods limits their applications [7]. Also, these methods generate harmful by-products such as contaminant-saturated adsorbents, sludges, or oxidizing substances [2].

✉ Bilgen Osman
bilgeno@uludag.edu.tr

Altynay Zhumabekova
502009015@ogr.uludag.edu.tr

Samir Abbas Ali Noma
snoma@uludag.edu.tr

Elif Tümay Özer
etumay@uludag.edu.tr

[1] Department of Chemistry, Faculty of Arts and Science, Bursa Uludag University, 16059 Gorukle, Bursa, Turkey

Published online: 13 February 2024

In recent years, enzymatic treatment of dyes has attracted significant attention. Enzymes are green biocatalysts that speed up biochemical reactions in living organisms [8]. They can act on specific pollutants to remove them by transforming them into other (innocuous) products or making them more convenient for further treatment [9]. Enzymatic treatment is more cost-effective and efficient than conventional treatment due to its environmental friendliness, ability to perform in mild conditions, high specificity and selectivity, and no toxic by-products during wastewater treatment [10]. Among the different enzymes applied for decolorizing and degrading dyes, peroxidases are promising candidates for industrial wastewater treatment due to their stability, low cost, and tolerance to wide temperature and pH ranges [11].

Horseradish peroxidase (HRP; EC 1.11.1.7) is a heme-containing oxidoreductase enzyme mainly extracted from horseradish plant root (Armoracia rusticana) [8]. It has a molecular weight of approximately 44 kDa [12]. HRP enzyme contains four disulfide bridges, 308 amino acids, oligosaccharides, ferroporphyrin, and two seven-coordinate calcium atoms, stabilizing its structure and property [13, 14]. Arg-38 and His-42 are involved in peroxidase catalysis [15–17]. A hydrophobic pocket acquired by His-42, Phe-68, Gly-69, Ala-140, Pro-141, Phe-142, and Phe-179, and heme methyl C18 is the reducing substrate-binding site of HRP and substrate oxidation occurs at the exposed heme edge, a region comprising the heme methyl C18 and heme meso C20 protons [15, 18–20]. Three functionally important COOH groups are of a protein nature. They are not directly involved in the enzyme-active site but are essential for the binding and oxidation of *o*-dianisidine [21]. It is receiving significant attention because of its broad substrate specificity, affordable price, and extraction convenience [22, 23]. It catalyzes the oxidation reaction of different substrates by degrading hydrogen peroxide (H_2O_2). Recently, HRP has been used to decontaminate hazardous compounds such as dyes, pharmaceuticals, phenols, xenobiotics [24]. However, HRP has disadvantages that limit its techno-commercial application, such as low stability, contamination of the final product, and difficulty in reuse.

To overcome these disadvantages, the immobilization process can be used. Enzyme immobilization is defined as the binding or trapping of free enzymes inside or on the surface of a solid carrier matrix, resulting in decreased mobility [25]. The immobilization process improves the enzyme's activity, stability, and reusability to be applied in different reaction environments and extreme conditions. The main immobilization methods are adsorption, entrapment, covalent attachment, and cross-linking [26]. The immobilization process should not modify the active site's chemical structure and reactive groups; therefore, it is vital to choose a suitable immobilization method to prevent activity loss [27]. The support material to be used in enzyme immobilization should be non-toxic, provide mass transfer with minimum diffusion resistance, and avoid enzyme aggregation and denaturation without disrupting the natural conformation of the enzyme [28].

Decolorization of azo dyes with immobilized HRP enzyme has attracted attention due to the applicability of HRP in wide temperature and pH ranges, stability, and low cost. Different supports have been used in HRP immobilization to meet requirements such as mass transfer and preservation of the natural enzyme conformation by preventing aggregation and disruption. This study aimed to immobilize HRP enzyme on poly(ethylene glycol dimethacrylate-*N*-methacryloyl-amido-L-tryptophan methyl ester) (PEDMT) microbeads by adsorption and to investigate the usability of immobilized-HRP enzyme (PEDMT–HRP) for decolorization of Congo red (CR) and Reactive Black 5 (RB5) solutions. The PEDMT microbeads were characterized via Brunauer–Emmett–Teller (BET) analysis, Fourier transform infrared spectroscopy (FTIR), scanning electron microscopy with energy-dispersive X-ray analysis (SEM/EDX), X-ray photoelectron spectroscopy (XPS), and X-ray diffraction (XRD) analyses. The efficiency of the free HRP and PEDMT–HRP was compared by elucidating the parameters affecting the immobilization. The effects of pH, temperature, substrate concentration, metal ions, organic solvents, and H_2O_2 concentration on the enzyme activity, the thermal and storage stability of the free and immobilized enzyme, and reusability of PEDMT–HRP were determined. Then, the effects of pH, dye concentration, amount of HRP-immobilized PEDMT microbeads and enzyme, H_2O_2 concentration, and contact time on the decolorization of CR and RB5 solutions were investigated. The reusability of the immobilized HRP in dye decolorization was also tested. HPLC analyses were conducted to determine the efficiency of PEDMT–HRP in the simultaneous decolorization of the dyes under optimum conditions.

2 Experimental

2.1 Materials

2.1.1 Reagents

L-tryptophan methyl ester hydrochloride, polyvinyl alcohol (PVA), EGDMA, RB5, and CR were obtained from Sigma-Aldrich. Methacryloyl chloride was obtained from Fluka. Triethylamine was obtained from Across Organics. N,N'-azobisisobutyronitrile (AIBN), and H_2O_2 were obtained from Merck. Horseradish peroxidase (EC 1.11.1.7) and *o*-dianisidine were obtained from Sigma Chem. Other chemicals and reagents employed were of analytical grade.

2.1.2 Synthesis and Characterization of the PEDMT Microbeads

PEDMT microbeads were produced via suspension polymerization of EGDMA with *N*-methacryloyl-amido-L-tryptophan methyl ester (MATrp) monomer as described in our previous study [29]. AIBN and PVA were the initiator and the stabilizer, respectively, and toluene was included in the polymerization steps as a pore former. The synthesis reaction of PEDMT microbeads is given in Fig. SI1.

2.1.3 Immobilization of HRP onto the PEDMT Microbeads

For the immobilization of HRP, PEDMT microbeads (100 mg) were mixed with 1U of HRP enzyme dissolved in acetate buffer (pH 6.0), then incubated, and stirred at 4 °C for 24 h. After 24 h, the mixture was centrifuged at 5000 rpm at 4 °C to separate and store the supernatant for the following experiments. The HRP-immobilized PEDMT microbeads were washed three times with distilled water to remove free enzyme molecules not adsorbed on the microbeads. Ultimately, it was left to dry overnight at room temperature and then kept in the refrigerator at 4 °C until subsequent application.

To quantitatively describe the effectiveness of immobilization, immobilization yield, activity yield, and immobilization efficiency were calculated via Eqs. (1), (2), and (3), respectively.

$$\text{Immobilization yield}(\%) = \frac{C_\text{i} - C_\text{s}}{C_\text{i}} \times 100 \tag{1}$$

here C_i is the initial concentration of enzyme; C_s is the total concentration of unbound enzyme in the supernatant and washing solutions.

$$\text{Activity yield}(\%) = \frac{A_\text{i}}{A_\text{f}} \times 100 \tag{2}$$

here A_i is the activity of immobilized HRP, and A_f is the activity of free HRP.

$$\text{Immobilization efficiency}(\%) = \frac{\text{Activity yield}}{\text{Immobilization yield}} \times 100 \tag{3}$$

2.2 Instrumental Measurements

The microbeads' average size and size distribution were determined by screen analysis performed with Tyler standard sieves (Retsch Gmbh; Haan, Germany). The PEDMT microbeads in the diameter range of 106–180 μm were used to prepare PEDMT–HRP. SEM–EDX analysis was used to determine microbeads' surface morphology and investigate the HRP enzyme's existence on the microbead's surface. FTIR analysis was performed with Perkin Elmer Spectrum 100 model FTIR instrument in the 400–4000 cm^{-1} frequency range. The microbeads' average pore size (nm), specific surface area (m^2/g), and total pore volume (cm^3/g) were determined by BET analysis with an ASAP2000 instrument (Micromeritics). P/P_o-V (cc/g) and pore diameter (Å)-dV(d) (cm^3/Å/g) graphs were prepared by using N_2 adsorption–desorption data obtained under vacuum at 77 K. The chemical compositions of the PEDMT and PEDMT-HRP microbead surfaces were analyzed using XPS Apparatus (PHI-5000) from PHI, USA. The experiment conditions are as follows: The energy of excitation source monochromatic Al Kα radiation was 1486.6 eV, and survey scan range was 0–1100 eV. The electron take off angle was fixed at 45°. After scanning the overall spectrum for 2–3 min, peaks over narrow ranges were recorded for C1*s*, O1*s*, N1*s* for 4–5 min. The PEDMT microbeads, PEDMT–HRP, and HRP enzymes were characterized by XRD patterns on a Bruker, D8 Discovery XRD diffractometer system.

Michaelis–Menten constant (Km) and maximum reaction rate (Vmax) were determined for free HRP and PEDMT–HRP. Initial velocities were measured by varying the substrate concentrations from 0.25 to 6 mM. Using the experimental data, Km and Vmax for free HRP and PEDMT-HRP were determined from Lineweaver–Burk plots.

2.3 Enzyme Activity Measurements

The total peroxidative activity of free HRP and PEDMT-HRP was colorimetrically measured using *o*-dianisidine as a substrate [30]. The assay mixture contained 5 mg of PEDMT–HRP or an equal amount of free HRP, *o*-dianisidine (6 mM, 2 mL) dissolved in phosphate buffer (pH = 6.0, 50 mM), and H_2O_2 (75 μL, 3% *v*/*v*, 22.05 μmol H_2O_2). The mixture was incubated in a water bath for 10 min at 40 °C; then, NaOH solution (1.5 M, 75 μL) was added to stop the reaction. HRP activity was evaluated by measuring the increase in the absorbance at 460-nm wavelength resulting from bisazobiphenyl that forms due to the oxidation and polymerization of *o*-dianisidine. One unit (1.0 U) of peroxidase activity is described as the amount of enzyme that catalyzes the oxidation of 1.0 μmol of *o*-dianisidine to the colored product in 1 min. All experiments were done in triplicate, and mean ± standard deviation values were calculated. The highest activity value was assumed as 100%, so results were evaluated relative to it and given as relative activity (%).

To investigate the reusability of PEDMT–HRP, the enzyme activity was measured repeatedly under optimum conditions. After each experiment, PEDMT–HRP was separated from the reaction medium by centrifugation and washed with buffer solution. So, the reaction was repeated with a

fresh substrate ten times under the same conditions. Initial enzyme activity was defined as 100%, and the following activities were calculated relatively.

2.4 Decolorization Studies

To evaluate the efficiency of free HRP and PEDMT–HRP in dye decolorization, CR and RB5 were used as model dyes. Stock dye solutions (500 mg/L) were prepared and used for further experiments by diluting. The wavelengths in which the maximum absorption occurred were detected by preparing UV spectra for dye solutions using a UV–VIS spectrophotometer (Shimadzu UV-1700). Calibration plots were prepared and used to determine the dye concentration during decolorization studies. The decolorization efficiency was calculated by Eq. (4).

$$\text{Decolorization}\ (\%) = \frac{\text{Initial dye concentration} - \text{Final dye concentration}}{\text{Initial dye concentration}} * 100 \quad (4)$$

2.5 Reusability Studies

The reusability of PEDMT–HRP on dyes decolorization was investigated for several sequential reactions. After each reaction cycle, the HRP-immobilized microbeads were collected by filtration and washed with phosphate buffer and then reused with a fresh dye solution. The assay was repeated for 10 cycles of CR and 5 cycles of RB5. The decolorization efficiency of the PEDMT-HRP enzyme in the first cycle was considered 100%, and the subsequent efficiencies were calculated as relative decolorization.

2.6 HPLC Analyses

To investigate the efficiency of immobilized HRP on decolorization, PEDMT–HRP was used for separate and simultaneous decolorization of CR and RB5 solutions under optimum conditions (5 mL of the dye solution (50 mg/L for CR and 25 mg/L for RB5) in PBS buffer (pH 6.0), 0.2 mL H_2O_2, 15 mg HRP-immobilized microbeads). The decolorization studies were also conducted by adding 0.4 mL free HRP solution to the dye solutions with the same volumes and concentrations. After 30-min incubation at 45 °C in all cases, the enzymatic reaction was stopped with 0.1 mL 1.5 M NaOH. Control samples run in parallel without adding PEDMT–HRP and free HRP. The adsorption capacities of the PEDMT microbeads for CR and RB5 were also determined by batch adsorption experiments at the same conditions of decolorization studies with the enzymes (5 mL of the dye solution (50 mg/L for CR and 25 mg/L for RB5) in PBS buffer (pH 6.0)/15 mg PEDMT microbeads/30-min incubation at 45 °C). CR and RB5 analyses were performed using an Agilent 1200 series HPLC system (Agilent, Palo Alto, CA) consisting of a G-1311A quaternary pump, a G-1329A ALS autosampler, a G-1322A degasser, and a G-1315B diode array detector (DAD) using Agilent Zorbax 300SB-C18 (250 mm 4.6 mm i.d., 5 μm) column. Elution was performed using a mobile phase consisting of a mixture of acetonitrile (A) and 10 mM ammonium acetate (CH_3COONH_4) solution acidified to pH 3.6 with acetic acid (CH_3COOH) (B) at isocratic mode. Before injection, the samples were filtered through 0.45-μm syringe PVDF filters. The decolorization ratio (%) was calculated using Eq. (4). All experiments were performed in triplicate, and the average of the replicates and standard deviation was determined.

3 Results and Discussion

3.1 Properties of the PEDMT Microbeads

SEM analyses were performed to examine the morphology of polymeric microbeads before and after immobilization. SEM images of the PEDMT and HRP-immobilized PEDMT microbeads obtained at different magnifications are given in Fig. 1. It can be seen that the prepared microbeads had a highly porous and spherical structure. SEM images taken at higher-magnification ratios illustrated that after immobilization, most of the pores were clogged, and there were bumps on the surface of microbeads (Fig. 1d and f). It can be assigned to the physical adsorption of HRP inside the pores and onto the surface of microbeads. Consequently, the surface morphology of PEDMT microbeads was changed after immobilization, demonstrating that HRP was successfully immobilized onto the PEDMT microbeads.

PEDMT and HRP-immobilized PEDMT microbeads were also subjected to EDX analysis to determine the elemental compositions of the microbeads' surfaces (Fig. SI2). The results demonstrated the presence of carbon, nitrogen, and oxygen in the chemical structure of PEDMT and HRP-immobilized PEDMT microbeads. However, the HRP-immobilized PEDMT microbeads had also sulfur (0.43%). Moreover, the nitrogen ratio increased from 2.26 to 3.5% after HRP immobilization. Overall, it can be concluded that the elemental composition changed after immobilization, demonstrating the success of the applied immobilization procedure.

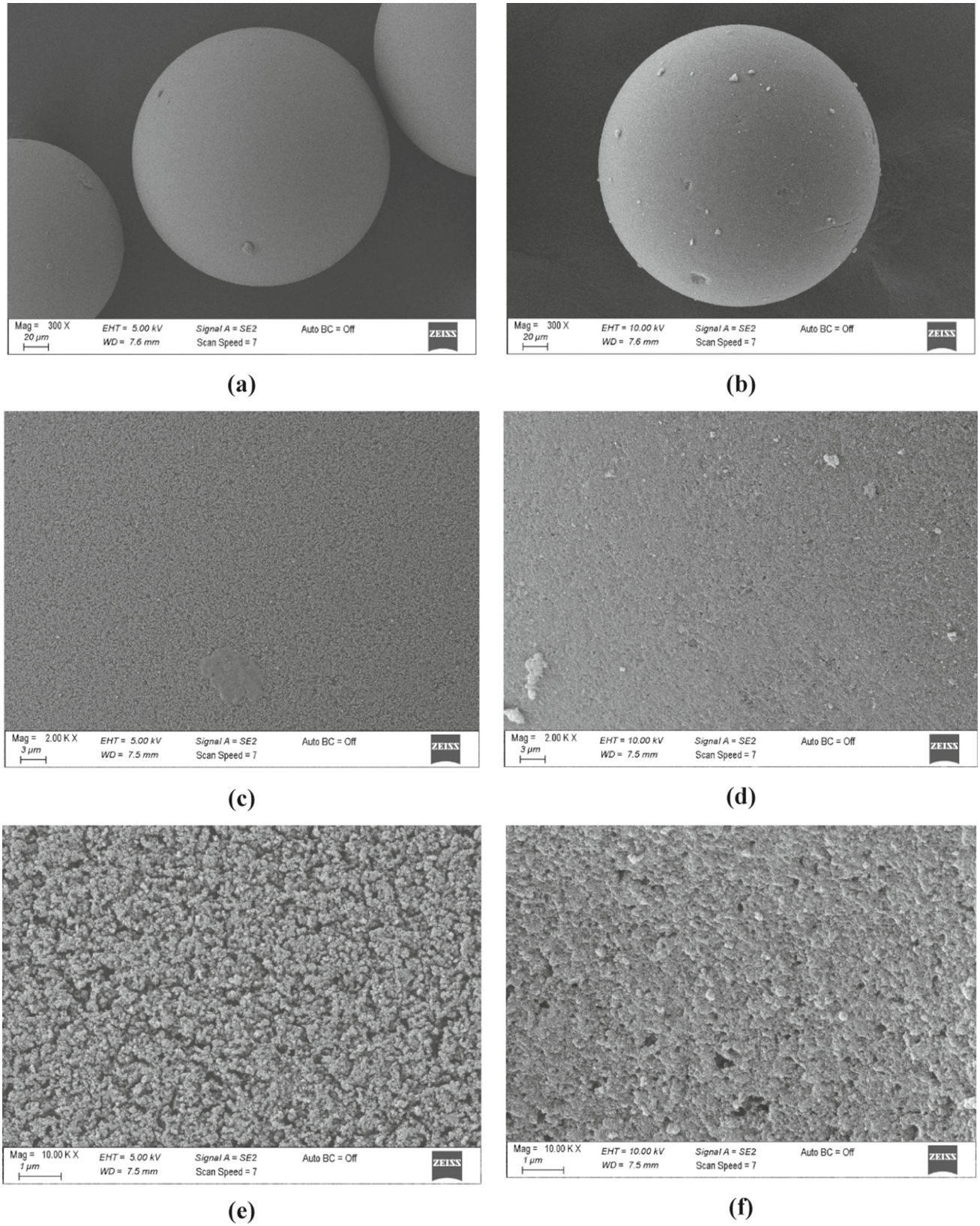

Fig. 1 SEM images of the PEDMT (**a**, **c**, **e**) and HRP-immobilized PEDMT (**b**, **d**, **f**) microbeads at different magnification ratios

FTIR spectra of the PEDMT microbeads, HRP enzyme, and PEDMT–HRP are given in Fig. SI3. For free HRP, the characteristic absorption bands at 1639 cm^{-1}, 1528 cm^{-1}, and 1387 cm^{-1} were attributed to the vibration of (–CONH–) amide I, amide II, and amide III, respectively. The observed absorption band at 3284 cm^{-1} was related to O–H vibration and 2934 cm^{-1} was associated with the alkyl group ($–CH_2$). Another absorption band at 1038 cm^{-1} corresponded to the aliphatic amines (C–N stretching). In the FTIR spectrum of PEDMT microbeads, absorption bands of the ester carbonyl group (C=O) at 1724 cm^{-1} and repeating aliphatic C–H bonds at 2952 cm^{-1} were observed. The spectrum of PEDMT–HRP still had the characteristic absorption band of the PEDMT microbeads, such as the ester carbonyl group at 1720 cm^{-1} and the aliphatic C–H bond at 2952 cm^{-1}. However, PEDMT–HRP had an additional absorption band at 1404 cm^{-1} assigned to NH (amide III) vibration. In addition, the FTIR spectrum of PEDMT–HRP consisted of absorption bands at 3422 cm^{-1} and at 1022 cm^{-1} belonging to O–H and C–N vibrations, respectively, similar to the spectrum of free HRP [31]. These results proved that HRP was successfully immobilized onto the PEDMT microbeads.

BET analysis was performed to describe the microbeads' surface's physical properties. The specific surface area, pore volume, and pore diameter of microbeads were determined via N_2 adsorption/desorption isotherms and pore diameter distribution graphs (Fig. SI4). The specific surface area of the PEDMT microbeads was very high (1103 $m^2\ g^{-1}$). The PEDMT microbeads had a pore volume and pore size of 1.94 $cm^3\ g^{-1}$ and 9.99–55.3 Å, respectively. It was clear that the microbeads had a highly porous structure and micro- and mesopores according to the IUPAC definition. High porosity and large surface area facilitated better HRP immobilization, which resulted in high enzymatic activity.

The full XPS spectra of the surfaces of PEDMT and HRP-immobilized PEDMT microbeads are given in Fig. SI5. The signal for N1*s* (400 eV) was not observed for PEDMT microbeads (Fig. SI5a). However, a signal for N1*s* (400 eV) in the XPS spectrum of HRP-immobilized PEDMT microbeads (Fig. SI5b), resulting from N atoms in the peptide bonds, demonstrated that the HRP enzyme was successfully adsorbed on the PEDMT microbeads. C1*s* (%), O1*s* (%), and N1*s* (%) were determined as 70.8%, 26.0%, and 3.1%, respectively. Figure SI6 shows the XRD spectra of PEDMT microbeads, PEDMT–HRP, and HRP enzymes. The obtained peaks showed that the microbeads and the enzymes have amorph structures. The XRD pattern of the PEDMT microbeads and PEDMT–HRP displayed a broad peak at 13.7° and 14.8°, respectively, in which a slight shift may result from the adsorption of HRP enzyme onto the microbeads.

3.2 Immobilization Parameters

Immobilization yield indicates the amount of enzyme that can bind to the support matrix [32]. Activity yield compares the activity of immobilized and free enzyme and shows a decrease in activity after immobilization. Immobilization efficiency represents two characteristics: first, the amount of immobilized enzyme, and second, the enzyme's activity in the carrier [33]. For this reason, parameters such as immobilization yield, activity yield, and immobilization efficiency for HRP immobilization on PEDMT microbeads were determined by incubating the microbeads with 1 U of HRP (pH 6.0, 4 °C, and 24 h). Immobilization yield was calculated as 84.9 ± 2.1%, activity yield as 73.8 ± 5.9%, and immobilization efficiency as 86.9 ± 6.9%. In a previous study, calcium alginate gel beads were used for HRP encapsulation, and immobilization efficiency was reported as 90% [22]. ZnO nanowires/macroporous SiO_2 composite was used as a support matrix for HRP immobilization, and immobilization efficiency was 75.3% [34]. In a recent report, the HRP enzyme was encapsulated via phospholipid-templated titania particles, and 70.51% immobilization yield and 56.31% activity yield were obtained [35]. As a result, it can be pointed out that obtained immobilization efficiency with the PEDMT microbeads was very high, probably due to the hydrophobic interactions between HRP enzyme, which is a protein, and the PEDMT microbeads including MATrp monomer, which is a derivative of hydrophobic amino acid tryptophan. The indole ring in the MATrp residue may interact with the hydrophobic amino acids' residues of HRP. In addition, hydrogen bonds may occur between C=O and –NH groups of MATrp residue and hydrogen donor and acceptor groups in the HPR protein.

3.2.1 Optimum pH and Temperature

One of the parameters that enzyme activity is affected is pH. The enzyme activity was measured in the pH range of 2.0 to 10.0 to determine the optimum pH. The assay mixture contained 5 mg of PEDMT–HRP or an equal amount of free HRP and was incubated in a water bath for 10 min at 40 °C. As seen in Fig. 2a, the maximum activities of free HRP and PEDMT–HRP were observed at pH 6.0. Similarly, in another study in which nanofibrous membranes were employed to immobilize HRP, the optimal pH value was found to be at pH 6.0 for both free and immobilized enzymes [36]. In another study, HRP was encapsulated by cyclodextrin nanosponge, and the maximum activity of free HRP was observed at pH 6.0. In contrast, the maximum activity of the encapsulated enzyme was observed at pH 7.0 [37]. The relative activity of PEDMT–HRP was higher and more stable in the comprehensive pH range than the free HRP. PEDMT–HRP showed 53% and 42% relative activity at pH 3.0 and 9.0, whereas free

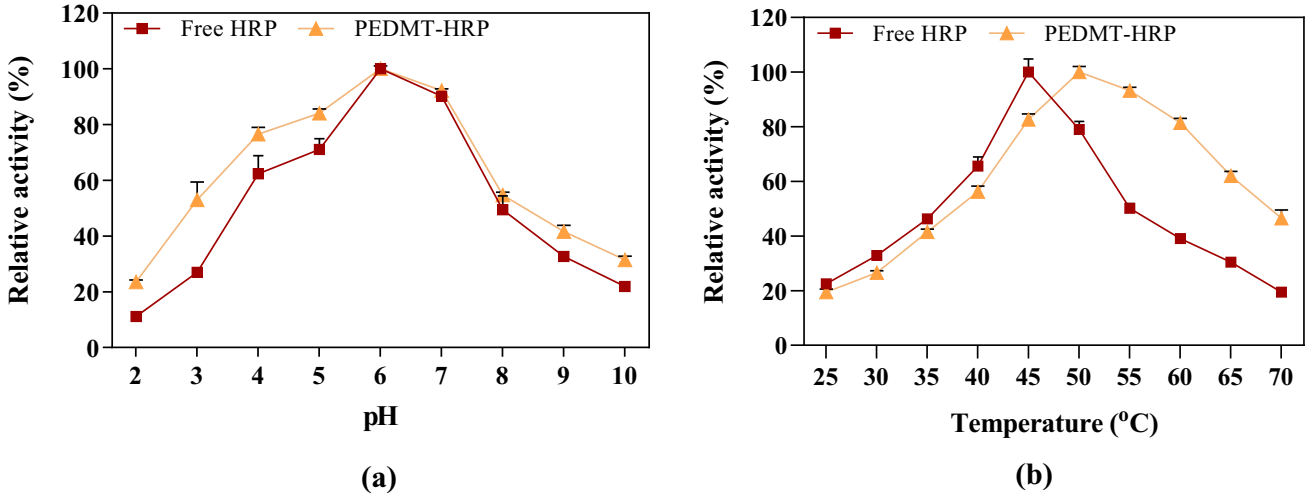

Fig. 2 **a** Optimum pH and **b** optimum temperature of free HRP and PEDMT–HRP

HRP showed 27% and 33% at the same pH values, respectively. PEDMT–HRP exhibited high pH resistance due to the stabilizing and protecting effect of the immobilization technique [35]. It illustrates that since HRP was immobilized with the adsorption method, there was no covalent bond between HRP and the PEDMT microbeads, and the optimum pH of the enzyme did not change after immobilization. Consequently, the immobilized PEDMT–HRP was marginally more stable than the free enzyme. The immobilized enzyme becomes more stable and less affected by environmental factors than the free enzyme; it makes them suitable for use in various fields [23, 38].

Another critical parameter for enzyme studies is to determine whether there are any changes in the optimum temperature after immobilization. The free HRP and PEDMT–HRP were incubated at 25 °C to 70 °C for 30 min. Then, the enzyme activity was assayed by using a substrate solution with the optimum pH value. The results are shown in Fig. 2b. The maximum activity of the free enzyme was obtained at 45 °C, while the PEDMT–HRP showed maximum activity at 50 °C. In a previous report, HRP was immobilized on activated wool. The optimum temperature for free HRP at 30 °C, whereas the optimum temperature for immobilized enzyme shifted to 40 °C [39]. In another study, Fe_3O_4 magnetic nanoparticles were used for HRP immobilization, and the optimum temperature of free HRP shifted from 40 to 50 °C for HRP immobilized on magnetic nanoparticles [40]. When the temperature was increased to 55 °C, the free HRP started to denature, whereas the PEDMT–HRP retained approximately 95% of its relative activity. Moreover, the free HRP was denatured at 70 °C, while PEDMT–HRP retained about 50% of its initial activity. These results showed that the PEDMT–HRP was stable over a broader temperature range and had a higher thermal resistance than the free HRP. This is because immobilization decreases the enzyme's thermal vibrations and stabilizes its conformational structure [13].

3.2.2 Optimum H_2O_2 Concentration

H_2O_2 is an essential co-substrate of the peroxidase enzyme that initiates a free radical reaction to form reaction intermediates and oxidizes the substrate [9]. For higher reaction efficiency, determining an optimal concentration of H_2O_2 in enzymatic reactions is vital. Because an excess amount of H_2O_2 inactivates the enzyme and an insufficient amount cannot provide enough oxidant [22], the enzymatic activity of HRP is due to the oxidation and reduction of the Fe^{3+} ion in the heme group. The catalytic reaction has two stages. In the first stage, H_2O_2 replaces the water ligand. Heterolytic break of the O–O bond allows H_2O_2 to react with the Fe^{3+} ion and form three products: H_2O, Fe^{4+} oxoferryl center, and a positively charged radical based on porphyrin. In the second stage, the positively charged porphyrin radical undergoes one-electron reduction or one-electron transfer reaction with chosen substrate: Fe^{4+} oxoferryl species, and the first radical of the substrate is obtained. Consecutively, it undergoes a reduction reaction with the substrate and returns to the initial form of the enzyme (Fe^{3+}); here, the second radical of the substrate is obtained. The obtained free-radical compounds of the substrate tend to polymerize, which is an advantage of the process. The oxidation reaction of HRP with aromatic compound (AH_2) in the attendance of H_2O_2 is $H_2O_2 + 2AH_2 \xrightarrow{HRP} 2H_2O + 2AH^{\cdot}$

To find the optimum H_2O_2 concentration, enzyme activities of free HRP and PEDMT–HRP were measured with different H_2O_2 concentrations (1–5%) under constant conditions, and the results are shown in Fig. SI7. The relative activity of both enzymes was increased with increasing H_2O_2

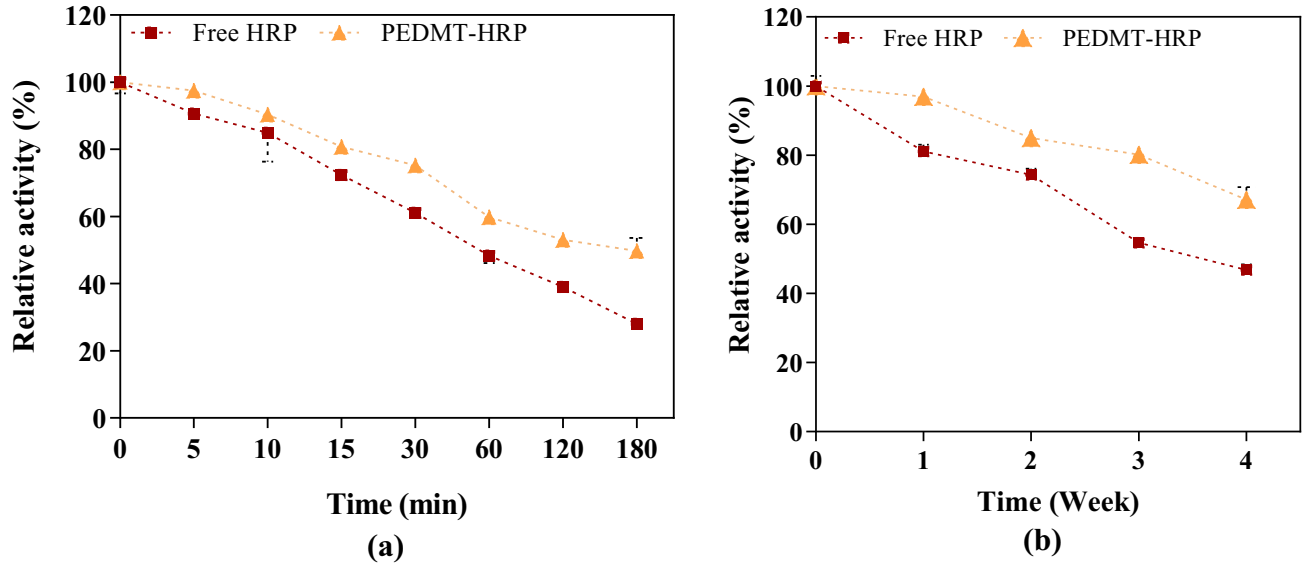

Fig. 3 **a** Thermal stability and **b** storage stability of free HRP and PEDMT–HRP

concentration. The maximum activity was obtained when the H_2O_2 concentration was 3% (*v*/*v*). With a further increase in the concentration, the activity of the free HRP continued to decrease, while the PEDMT–HRP's activity was stabilized.

3.2.3 Thermal and Storage Stability Properties

Thermal stability is one of the most significant superiors of immobilized enzymes as per free enzymes. The immobilization process makes enzymes more resistant to environmental conditions, including intense heat; it is advantageous for commercial use [12]. Thermal stability is a parameter that evaluates the ability of enzymes to remain active at elevated temperatures. Figure 3a shows the thermal stability of both free HRP and PEDMT–HRP. After 3-h incubation at 50 °C, free HRP lost most of its initial activity, and only 28% of initial activity remained, while the PEDMT–HRP protected more than 50% of the initial activity. During the reaction, the activity of PEDMT–HRP dropped less and slowly compared to free HRP. In an early study, HRP was immobilized on poly(ethylene terephthalate) grafted acrylamide fiber. The thermal stabilities were investigated by incubating both enzymes for 180 min at 50 °C. The results showed that the immobilized HRP retained 44% of its initial activity, whereas the free HRP retained only 19% [41]. This improvement in temperature resistance may be due to reduced enzyme mobility and high conformational integrity after immobilization. These results show that immobilization significantly improves thermal stability, promising the enzyme to be used even at high temperatures where the free enzyme is very unstable.

Storage stability is a significant parameter for the commercial-scale application of the enzymes. It is well known that the enzyme in solution is unstable during storage, and its activity decreases spontaneously over time. Therefore, the storage stability of both free HRP and PEDMT–HRP was investigated at room temperature for 4 weeks. As seen in Fig. 3b, free HRP showed a downward trend over time. After 4 weeks, the activity PEDMT–HRP was still above 67% of the initial activity, while the free HRP retained only 47% of the initial activity. In a recent study, carboxyl-functionalized polystyrene [poly(styrene-co-methacrylic acid)] nanofibers were used as a matrix for HRP immobilization. After 20 days of incubation, the activity for immobilized-HRP was still above 60% from the initial activity and nearly 35% for free HRP [36]. In another work, silica hollow fibers were used for immobilizing the HRP enzyme. After 1 week of storage, the activity for immobilized-HRP was still above 60%, but free HRP was above 41% [42]. The free enzyme's stability is lower because it is easily affected by environmental conditions. However, immobilized enzymes adapt better to environmental conditions than free enzymes due to their stable conformational state and strong interactions with the carrier matrix [43]. Loss of enzymatic activity during this period can be attributed to protein denaturation and degradation during long-term storage. The results showed that immobilization of HRP onto the PEDMT microbeads increased the stability of the HRP enzyme.

3.2.4 Effects of Metal Ions and Organic Solvents

Metal ions contribute to the catalytic process through their ability to attract or donate electrons. Some metals bind the

substrate by coordination links. Others contribute to maintaining the tertiary and quaternary structures of the enzyme molecule. Enzyme samples were incubated with different metal ion solutions to evaluate the effect of metal ions on the activity of free HRP and PEDMT–HRP. The relative activity was then measured at optimum conditions. The results obtained are shown in Fig. SI8a. It was determined that Ag^{+}, Cu^{2+}, and Fe^{3+} caused an increase in the activity of both free and immobilized enzymes, increasing by 16%, 30%, and 45% with free HRP and by 62%, 65%, and 93% with PEDMT–HRP, respectively. However, in the presence of other metal ions (Ca^{2+}, Co^{2+}, Mg^{2+}, Ni^{2+}, Sc^{3+}, Zn^{2+}, and Pb^{2+}), free HRP lost its activity, while PEDMT–HRP, on the contrary, gained a significant amount of activity. In a recent study, Fe^{2+} and Cu^{2+} had strong activation for immobilized HRP compared to soluble HRP. Other metals tested had less inhibitory effect on immobilized HRP than on soluble HRP [40, 44]. The metal ions are classified as soft, borderline, and hard. They present different binding characteristics for amino acids in the protein structure, i.e., hard metal ions (Ca^{2+}, Mg^{2+}, Sc^{3+}, Fe^{3+}) bind to O donor atoms of amino acids such as Asp and Glu and soft/borderline metal ions (Ag^{+}, Co^{2+}, Ni^{2+}, Cu^{2+}, Zn^{2+}, and Pb^{2+}) bind to N and S donor atoms of amino acids such as His and Cys. In this study, Ag^{+}, Cu^{2+}, and Fe^{3+} caused an increase the activity of both enzymes (free and immobilized) binding via O, N, and S donor atoms of the amino acids. On the other hand, the other metal ions (Co^{2+}, Ca^{2+}, Mg^{2+}, Ni^{2+}, Sc^{3+}, Zn^{2+}, and Pb^{2+}) caused a decrease in the activity of only free HRP enzyme via binding to O, N, and S atoms of amino acid, which probably essential to maintain of the native conformation. However, in the immobilized HRP, there was no activity decrease probably because the immobilization increased the stability of native conformation due to the binding to a polymeric support. As a result, it can be reported that any metal ions did not inhibit PEDMT–HRP compared to free HRP, and its activity was higher. This stability is due to the most significant advantage of the immobilization method, which is least affected by environmental factors.

The effect of various organic solvents on free HRP and PEDMT–HRP activity was also investigated and is shown in Fig. SI8b. Mixing organic solvents with water leads to many exciting variations and possibilities depending upon the miscibility of the solvent with water and the relative proportion of the solvent and water in the medium. The organic solvents have been found to profoundly affect enzyme catalysis, affecting both reaction rate and selectivity. The results showed that both enzymes were not inhibited only by ethanol and DMSO solvents. DMSO increased the activity of the free HRP and PEDMT–HRP by approximately 4% and 24%, respectively. In comparison, ethanol caused an increase in PEDMT–HRP's activity by 14% but did not significantly change the free enzyme's activity by only 2%. Other solvents, such as dichloromethane, toluene, diethyl ether, chloroform, and benzene, caused a decrease in the activity of free HRP and PEDMT–HRP. However, the activity of the PEDMT–HRP was relatively higher, and it was not affected by the solvents as much as the free enzyme. When an enzyme is placed in a non-aqueous medium, it is exposed to different factors that can change its aqueous-based native structure and, consequently, its function, presenting larger Km values [45]. The theoretical kinetic model developed by Lee and Kim [46] showed that enzyme reaction rate in organic media depended mainly upon substrate solvation and enzyme hydration. Any alteration in the enzyme's structure upon hydration causes a change in Km [45], whereas the maximum reaction rate is independent of the medium composition [47]. This is because the substrate and water's activity coefficients determine the enzyme reaction rate in organic solvents. Enzymes that require fewer water molecules have a higher reaction rate in organic media [46]. Therefore, the reaction rate was closely related to the polarity index of the organic solvent. The order of polarity index of organic solvent is DMSO > ethanol > dichloromethane > diethyl ether > chloroform > benzene > toluene. The results showed that low polarity index solvents (dichloromethane, diethyl ether, chloroform, benzene, and toluene) caused a decrease in the activity of free HRP. In contrast, DMSO and ethanol caused an increase in the activity of free and immobilized HRP. Dichloromethane, diethyl ether, chloroform, benzene, and toluene did not significantly change the activity of immobilized HRP due to the stability of the HRP enzyme obtained via immobilization.

3.2.5 Reusability of the PEDMT–HRP

Reusability is one of the immobilized enzyme's most significant advantages over the free enzyme for industrial applications. Therefore, the reusability of the PEDMT–HRP was investigated, and the results are shown in Fig. 4. The results showed that immobilized enzyme preserved more than 55% of its initial activity even after 10 consecutive uses. It proved that the PEDMT–HRP was suitable for reuse. In a recent study, the activity of immobilized HRP was tested for 5 successive cycles, and the enzyme retained approximately 40% of its initial activity [48]. On the other hand, HRP was immobilized on poly(methyl methacrylate) nanofibers incorporated with nanodiamonds, and the activity remained above 60% of its activity even after 10 consecutive cycles [49]. A decrease in activity may have occurred due to enzyme leakage or disruption of protein conformation [13]. Free enzymes are easily denatured and used only once, whereas immobilized enzymes can be separated from the reaction medium and used many times. Reusability also reduces the cost of immobilized enzymes and prevents side effects [50, 51]. As a result, the PEDMT–HRP can be reused effectively,

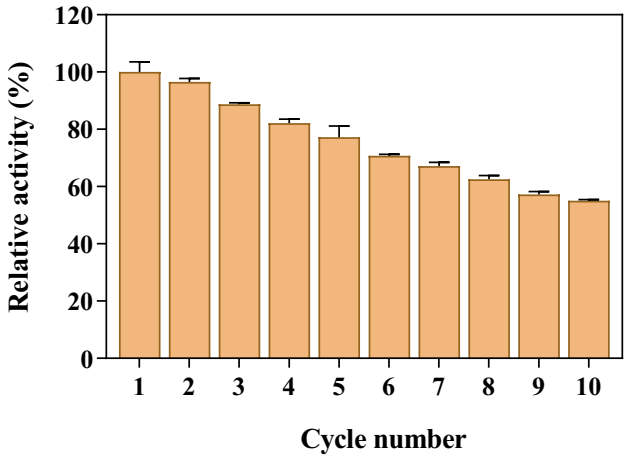

Fig. 4 The reusability of PEDMT–HRP

demonstrating that it has potential for application in the industry.

3.2.6 Kinetic Parameters

The effect of different substrate concentrations on free HRP and PEDMT–HRP reaction rate was determined from Lineweaver–Burk plots shown in Fig. SI9. The maximum rate of an enzymatic reaction (*V*max) was decreased after immobilization from 0.23 to 0.05 μmol/min. Similarly, the substrate concentration that allows reaching half of the maximum velocity (Km) has decreased after immobilization from 3.66 to 0.76 mM. The Km value dropped after immobilization due to increased substrate diffusional constraints. In another study, hydrazine-treated acrylic fabrics activated with cyanuric chloride were developed as supporting material for HRP immobilization. The results showed that increase in Km value after immobilization from 32.36 to 37.45 mM [44]. Also, in recent work, HRP immobilization onto functionalized superparamagnetic iron oxide nanoparticles was studied, and Km was increased after the immobilization of the HRP enzyme [23]. The Km value of the HRP enzyme decreased after being immobilized on PEDMT polymeric microbeads. Generally, it can be described as the immobilized enzyme's conformation change when bound to the microbeads [52]. In the meantime, a reduction in the *V*max value was detected following the immobilization of HRP. Limiting substrate diffusion to PEDMT–HRP may cause a decrease in *V*max. These outcomes result from modifications of enzyme structure after immobilization. This suggested that the rate of substrate-to-product conversion had decreased by decreasing the structural flexibility of the immobilized form, which led to a decrease in the affinity of the substrate to the enzyme active region [53].

3.3 Decolorization of CR and RB5 Dye Solutions

3.3.1 Effect of pH on Dye Decolorization

The change in pH impacts numerous functional groups, including amino and carboxyl on the surface, which influences the efficacy of dye decolorization, which control how dye molecules adhere to one another [54, 55]. Textile wastewater can have a broad range of pH values. Therefore, it is essential to ensure that the prepared PEDMT–HRP demonstrates high activity under acidic, basic, and neutral conditions [2]. Figure 5 shows the effect of pH on the enzymatic decolorization of CR and RB5 solutions. It was found that both free HRP and PEDMT–HRP showed the best decolorization at pH 6.0 for CR and RB5, which was also the optimum pH for HRP enzyme activity. At pH 6.0, the shape and functionality of the active site of HRP and immobilized HRP enzymes are optimum. On the other hand, CR, a dipolar molecule, is cationic at lower pHs and anionic at higher pHs. The pKa value of CR is 4.9 [56], and at pHs higher than 4.9, sulfo groups of the CR have a negative charge (SO_3^-), and amino groups (NH_3^+) have a positive charge. At pH 6.0, the net charge was near zero, increasing the affinity of the CR molecules to the hydrophobic reducing substrate-binding site, including His-42, Phe-68, Gly-69, Ala-140, Pro-141, Phe-142, and Phe-179, and heme methyl C18. However, RB5 has pKa values lower than zero due to their two sulfonate groups and another two sulfato-ethyl-sulfone groups, with negative charges even in highly acidic solutions [57]. As a result, PEDMT–HRP showed high decolorization percentages for CR at 89% and RB5 at 84%. In comparison, free HRP showed 48% for CR and 43% for RB5. As demonstrated, in contrast with free HRP, PEDMT–HRP can decolorize CR and RB5 more efficiently by 41% over a broader pH range from 6.0 to 8.0, providing an advantage for using PEDMT–HRP in the industry.

3.3.2 Effect of Dye Concentration on Decolorization

The influence of dye concentration on the enzyme's decolorization capacity was investigated, and the results are shown in Fig. 6. The highest dye decolorization for free HRP and PEDMT–HRP was achieved at 50 mg/L and 25 mg/L concentration for CR and RB5 solutions, respectively. Decolorization gradually decreased with increasing dye concentration. Decolorization resulted from degraded dyes by the HRP enzyme because the dye works as a second substrate. The increase in substrate concentration leads to an increased reaction rate until it achieves its maximum activity after the active center is full with the substrate; further addition of substrate will no longer affect the reaction rate [9]. Consequently, the decolorization (%) decreased as

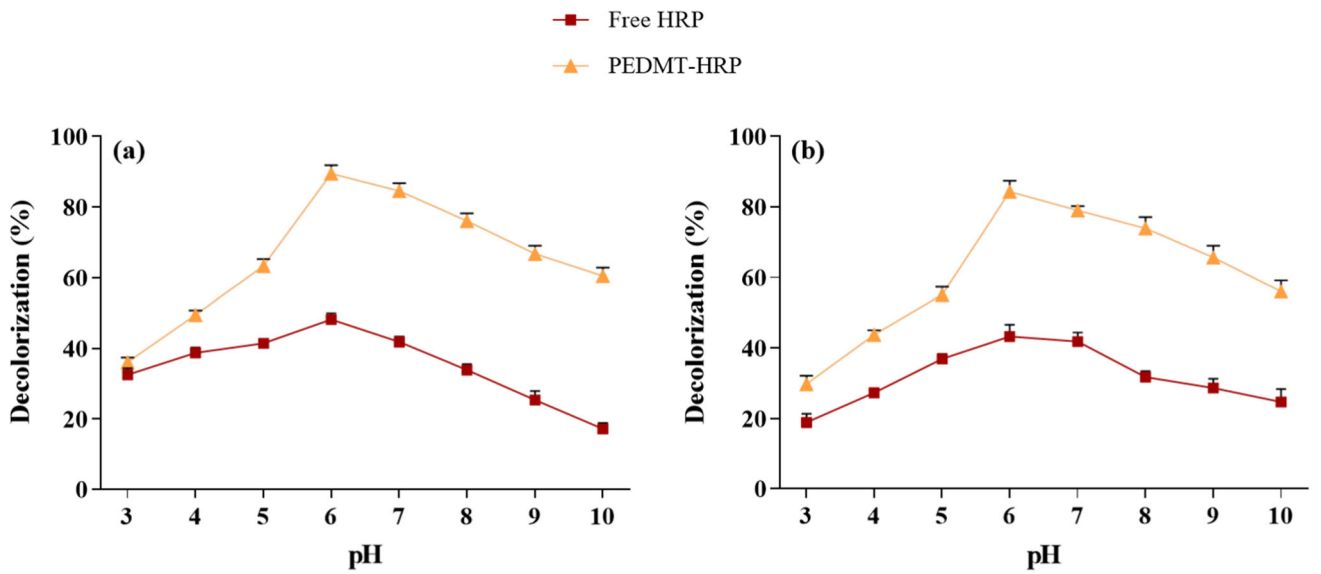

Fig. 5 Effect of pH on decolorization of **a** CR and **b** RB5 solutions (CR and RB5 concentration: 20 mg/L, PEDMT–HRP amount: 50 mg, HRP solution volume: 150 μL, temperature: 25 °C, time: 2 h, H_2O_2 concentration: 3%, *v*/*v*)

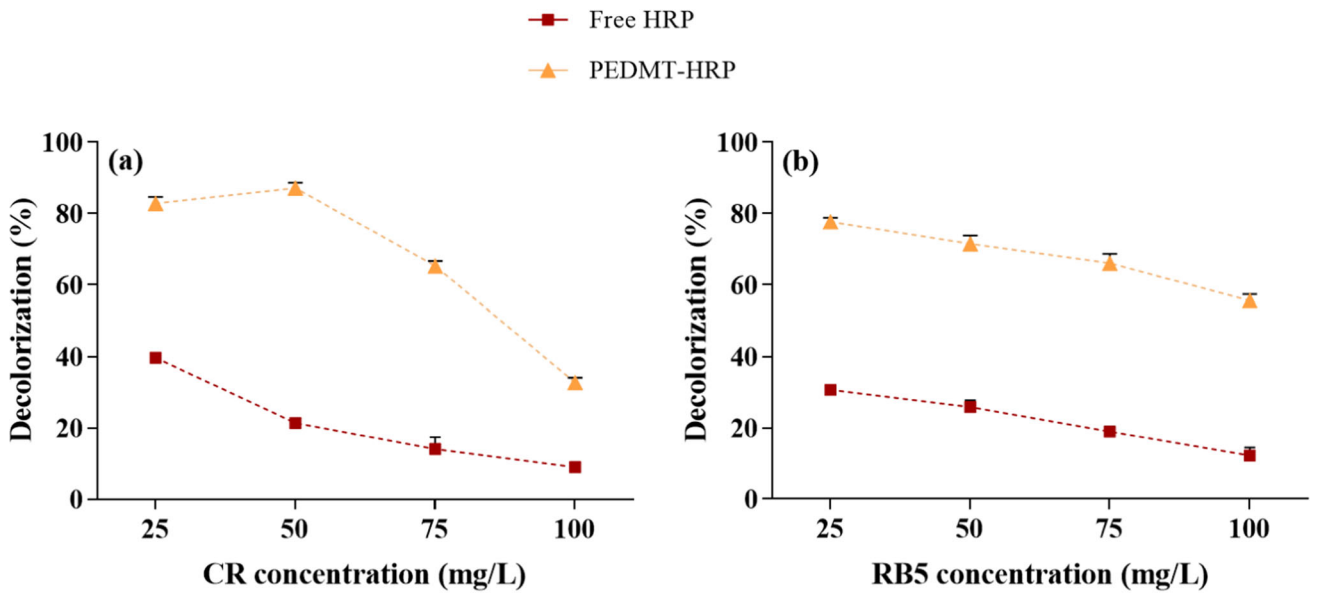

Fig. 6 Effect of dye concentration on decolorization of **a** CR and **b** RB5 solutions. (pH: 6.0, PEDMT–HRP amount: 50 mg, HRP solution volume: 150 μL, temperature: 25 °C, time: 2 h, H_2O_2 concentration: 3%, *v*/*v*)

the dye concentration increased. Under established experimental conditions, 50 mg/L and 25 mg/L concentration for CR and RB5 solutions are the limiting dye concentrations for optimal decolorization, respectively.

3.3.3 Effect of Enzyme Amount on Decolorization

Enzymes have a limited lifetime; therefore, enzymatic decolorization reactions directly depend on the amount of enzyme [9]. Figure SI10 represents the effect of the amount of free HRP and PEDMT–HRP for dye decolorization. In the experiments, 10 to 100 mg of PEDMT–HRP was used, while 50–300 μL of free HRP solution was used as an equal amount of PEDMT–HRP. The results showed the increase in the amount of PEDMT–HRP from 10 to 50 mg and free HRP concentration from 50 to 150 μL contributed to a tremendous increase in the percentage of decolorization of CR by 47% with PEDMT–HRP and 16% with free HRP and for RB5 by 39% with PEDMT–HRP and 19% with free HRP. However, the further increase in the amount of free HRP and PEDMT–HRP did not make a significant change in dye

decolorization. Therefore, 50 mg of PEDMT–HRP and 150 μL of free HRP solution were assumed to be the optimum enzyme amount at formulated experimental conditions.

3.3.4 Effect of H_2O_2 Concentration on Decolorization

Since H_2O_2 is required for the catalysis of HRP, the amount of H_2O_2 is critical for dye decolorization by free HRP and PEDMT–HPR [2]. Figure SI11 represents the dependence of CR and RB5 decolorization effectiveness on H_2O_2 concentration. The highest dye decolorization ratio by free HRP for 36% for both dyes (CR and RB5) was obtained at 3% of H_2O_2, while for PEDMT–HRP dye decolorization ratio reached 91% for CR and 81% for RB5 also was at 3% of H_2O_2. The molar ratio of H_2O_2/dye (CR and RB5) was 76 and 109.2 for CR and RB5, respectively. In comparison, 1% H_2O_2 gave the lowest dye decolorization efficiency for both dyes. The optimum H_2O_2 concentration depends on the initial dye concentration and differs from case to case. The behavior of the dye removal efficiency was similar in many dye types. First, the amount of dye removed sharply increased with an increase in hydrogen peroxide up to an optimal point. It shows that hydrogen peroxide is a limiting factor in this range. Second, after dye conversion reached its optimum point, adding hydrogen peroxide significantly reduced the conversion. An excess amount of hydrogen peroxide results in higher concentrations of intermediate products, which inhibit the enzyme's activity, and that enzyme is inactivated by an excess of hydrogen peroxide. The dye decolorization increased as the H_2O_2 concentration increased, and it dropped as the H_2O_2 amount was exceeded, owing to the inhibition of HRP activity by high H_2O_2 concentration [58]. The identical optimum H_2O_2 concentration (3%) was suggested by Kurtuldu et al., where HRP was adsorped onto UiO-66-NH_2 and used in Methylene Blue and Methyl Orange decolorization [59]. As a result, the immobilized enzyme could effectively decolorize both dyes over a broader H_2O_2 concentration range, demonstrating that PEDMT–HRP has greater tolerance to H_2O_2 than free HRP.

3.3.5 Effect of Contact Time on Decolorization

Identifying the optimum contact time helps to achieve the best decolorization efficiency within the shortest period and thus reduces process consumption and cost. After 2 h of incubation, no more dye decolorization was observed for both dyes. Figure SI12 illustrates the effect of reaction time on CR and RB5. For the free HRP, the maximum decolorization was 31% for CR and 34% for RB5 and achieved after 120 min of reaction. On the other hand, PEDMT–HRP showed efficient decolorization in 60 min but reached its maximum efficiency after 120 min of incubation. The maximum decolorization was 83% for CR and 82% for RB5. The same optimum reaction time of 120 min was presented by Karim et al. [1]. They immobilized the HRP enzyme by cross-linking onto the β-CD-chitosan complex and applied the immobilized enzyme in the decolorization of the mixture of Cypress Green and Sultan Red. Farias et al. [60] immobilized the HRP enzyme by calcium alginate gel beads through encapsulation and applied the immobilized HRP enzyme for dye decolorization. The optimum contact time for decolorization of Reactive Blue 221 and Reactive Blue 198 was 180 min and 240 min, respectively.

3.3.6 Reusability of PEDMT–HRP for Decolorization

The reusability of enzymes is an important index used for the evaluation after immobilization. As shown in Fig. 7, the reusability of PEDMT–HRP was evaluated via decolorization of two dye solutions. The PEDMT–HRP retained 89% and 27% of its initial activity after three repeated cycles with CR and RB5, respectively. PEDMT–HRP saved 44% after 10 cycles for CR decolorization while saving 17% of its initial activity after 5 cycles for RB5 decolorization. The above results could be due to the denaturation of the enzyme proteins that leads to its inactivation and leakage of the protein from the support material during use. Therefore, the PEDMT–HRP could serve its purpose in industrial applications, resulting in its reusability and easy recovery. In a previous study, HRP entrapped and cross-linked onto Na-alginate saved 74% of its initial activity after 10 reuse cycles with Acid yellow 11 [12]. In recent work, HRP immobilized on magnetic Fe_3O_4 and amino-functionalized magnetite nanoparticles, retaining 55% and 68% of its initial activity after 10 and 9 consecutive cycles, respectively [40]. Generally, the results proved that PEDMT–HRP displayed fairly good reusability compared to the literature, and it is a successful biocatalyst with reliable operational stability.

3.3.7 Decolorization Efficiency Under Optimum Conditions

The decolorization efficiency of CR under the optimum condition is shown in Fig. SI12. The experimental results in Fig. SI13a clearly showed that the decolorization efficiency for CR by free HRP reached 21.23% and by PEDMT–HRP reached 98.20% after 30 min at pH 6.0 and 45 °C. The adsorptive removal of CR by PEDMT microbeads reached 64.73% under optimum conditions. The decolorization efficiency for RB5 by free HRP and PEDMT–HRP was 1.04% and 47.99%, respectively. The removal ratio of RB5 by PEDMT microbeads was 9.65% after 30 min at pH 6.0 and 45 °C (Fig. SI13b). The decolorization effect of the PEDMT–HRP on the dyes was better than those of free HRP and adsorption via PEDMT microbeads.

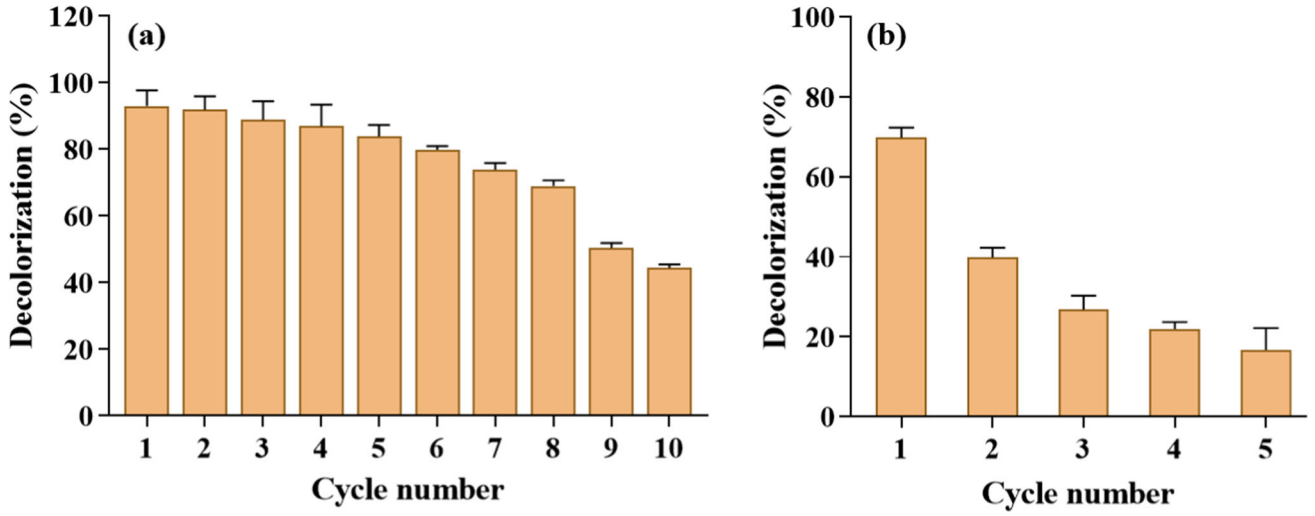

Fig. 7 Reusability of PEDMT–HRP in decolorization of **a** CR and **b** RB5 solutions

The results for simultaneous decolorization of the dyes with free HRP, PEDMT microbeads (adsorptive removal), and PEDMT–HRP are given in Fig SI13c. The PEDMT–HRP was importantly more effective than free HRP in simultaneous decolorization. Moreover, the adsorptive removal ratios of the dyes were significantly lower than enzymatic decolorization via PEDMT–HRP. As a result, the synergistic effect of adsorption and enzymatic degradation achieved rapid dyes degradation by shortening the mass transfer distance, and the simultaneous degradation rate of the dyes (CR and RB5) in 30 min exceeded 94% and 29%, respectively [61]. A comparison of the efficiency of immobilized HRP enzymes for dye decolorization is given in Table 1.

4 Conclusions

In this study, HRP enzyme was immobilized onto cross-linked polymeric microbeads (PEDMT) via adsorption, and the factors affecting the immobilization process were elucidated in detail. Then, the immobilized HRP enzyme (PEDMT–HRP) was used to decolorize CR and RB5 dye solution. The parameters affecting the decolorization efficiency were also studied. The microbeads were characterized by BET, SEM–EDX, and FTIR analyses. BET analysis showed that the PEDMT microbeads had a high surface area and pores in micro- and mesosizes. The PEDMT microbeads' surface was rough, increasing the surface area for HRP adsorption. Immobilization yield , activity yield, and immobilization efficiency were calculated as 84.9 ± 2.1, 73.8 ± 5.9%, and 86.9 ± 6.9%, respectively. The optimum pH was 6.0 for free and immobilized HRP, and the PEDMT–HRP was marginally more stable than the free HRP in a broader pH range. The optimum temperature was 45 °C for PEDMT–HRP, 5 °C higher than the free HRP. When the enzymes were incubated for 180 min at 50 °C, PEDMT–HRP retained 44% of its initial activity, whereas the free HRP had only 19%. The activity PEDMT–HRP was above 67% of the initial activity, while the free HRP retained only 47% for 4 weeks of storage. The PEDMT–HRP has significantly higher stability against metal ions and organic solvents and preserved more than 55% of its initial activity even after 10 consecutive uses. The *V*max and Km values of the HRP enzyme were decreased after immobilization. The optimum decolorization pH, H_2O_2 concentration, contact time, and HRP-immobilized microbeads amount were 6.0, 3% (*v*/*v*), 120 min, and 50 mg for both dyes. The highest decolorization was achieved at 50 mg/L and 25 mg/L concentrations for CR and RB5 solutions, respectively. The PEDMT–HRP saved 44% of its initial activity after 10 cycles for CR decolorization while preserving 17% of its initial activity after 5 cycles for RB5. HPLC analyses showed that the decolorization efficiency of CR and RB 5 by immobilized enzyme reached 98.20% and 47.99% after 30 min at pH 6.0 and 45 °C. The PEDMT–HRP could simultaneously decolorize both dyes with 94% (CR) and 29% (RB5) efficiency. Consequently, the PEDMT–HRP has application potential in the industry for decolorizing synthetic dyes.

Table 1 Comparison of the efficiency of immobilized HRP enzymes for dye decolorization

Immobilization method/support	Applications	Optimum dye decolorization pH	Optimum dye concentration (mg/L)	Optimum enzyme dose	Optimum H_2O_2 concentration	Optimum contact time	Decolorization efficiency, %	Reusability	Reference
Cross-linking/β-CD-chitosan complex	Mixture of 0.5% Cypress Green, 1.5% Sultan Red	8.0	–	0.2 U/mL	0.6 mM	2 h	83%	69% efficiency after 5 reuse	[1]
Acrylamide gel and alginate	Acid Black 10 BX	2.0	30	2.205 U/mL	0.6 µL/L	45 min	Acrylamide gel 79%, Alginate 54%	–	[9]
Entrapment and cross-linking/Na-alginate	Acid Yellow 11	5.0	–	0.0033 mg/mL	0.3 mM	12 min	> 99%	74% efficiency after 10 reuse	[12]
Adsorption and covalent immobilization/polyamide six electrospun fibers	RB 5 and Malachite Green	7.0	5	–	0.5 mM	1 h	Reactive Black 5 69%, Malachite Green 83%	–	[13]
Cross-linking/ZnO nanowires/macroporous SiO_2 composite	Acid Blue 113, Acid Black 10 BX	3.0/7.0	50	107.5 mg/g-support	–	35 min	Acid Blue 113 92.6%, Acid Black 10 BX 83.2%	79.4% efficiency after 12 reuse	[34]
Adsorption/kaolin	C.I. Acid Violet 109	5.0	40	0.1 IU	0.2 mM	40 min	87%	35% efficiency after 7 reuse	[38]
Encapsulation/calcium alginate gel beads	Reactive Blue 221, Reactive Blue 198	5.5	–	0.120 g	43.75 µM/37.5 µM	180 min/240 min	Reactive Blue 221 93%, Reactive Blue 198 75%	15% efficiency after 3 reuse	[60]
Entrapment/chitosan beads	Congo Red, Remazol Brilliant Blue R, RB 5, and Crystal Violet	5.0	–	5.0 g	–	2.0 mL/min	Congo Red 94.35%, Remazol Brilliant Blue R 82.17%, RB5 97.82%, and Crystal Violet 87.43%	64.9% efficiency after 6 reuse	[62]

Table 1 (continued)

Immobilization method/support	Applications	Optimum dye decolorization pH	Optimum dye concentration (mg/L)	Optimum enzyme dose	Optimum H_2O_2 concentration	Optimum contact time	Decolorization efficiency, %	Reusability	Reference
Adsorption/Fe_3O_4	Congo Red, Acid Violet 17, Rhodamine B, and Methylene Blue	7.0	25	50 mg/g for Congo Red, 35.2 mg/g for Acid Violet 17, 42 mg/g for Rhodamine B, 47.1 mg/g for Methylene Blue	–	10.5 h	Congo Red 99%, Acid Violet 17 90%, Rhodamine B 92%, Methylene Blue 98%	–	[63]
Covalent bonding/two ReliZyme™ supports (HFA 403 and EP 403)	Amido Black 10, Acid Orange 7, Direct Green, Methylene Blue, Acid Red, Neutral Grey	5.0–6.0	–	–	1.43 mM	30 min	> 99%	80% efficiency after 10 reuse	[64]
PEDMT–HRP	CR RB5	6.0	25	50 mg	3%,*v*/*v*	120 min (25 °C)	CR 98.20% (30 min,45 °C) RB5 47.99% (30 min, 45 °C)	44% efficiency after 10 cycles for CR 17% efficiency after 5 cycles for RB5	This study

Supplementary Information The online version contains supplementary material available at https://doi.org/10.1007/s13369-024-08748-6.

Acknowledgements This work was supported by the Research Foundation of Bursa Uludag University (Project No: FGA-2022-1226).

Author Contributions AZ involved in investigation, data curation, writing—original draft. SAAN took part in conceptualization, methodology, writing—review & editing. ETÖ took part in investigation, data curation, writing—original draft. BO took part in supervision, validation, writing—review & editing, funding acquisition, project administration.

Funding Open access funding provided by the Scientific and Technological Research Council of Türkiye (TÜBİTAK). This work was supported by Bursa Uludag University (Project Number: FGA-2022-1226).

Data Availability The supporting information file includes all data.

Declarations

Conflict of interest The authors have no relevant financial or non-financial interests to disclose.

Consent for Publication All authors consented to this publication.

References

1. Karim, Z.; Adnan, R.; Husain, Q.: A β-cyclodextrin–chitosan complex as the immobilization matrix for horseradish peroxidase and its application for the removal of azo dyes from textile effluent. Int. Biodeterior. Biodegrad. **72**, 10–17 (2012)
2. Jin, X.; Li, S.; Long, N.; Zhang, R.: A robust and stable nano-biocatalyst by co-immobilization of chloroperoxidase and horseradish peroxidase for the decolorization of azo dyes. J. Chem. Technol. Biotechnol. **93**, 489–497 (2018)
3. Zare, K.; Sadegh, H.; Shahryari-Ghoshekandi, R.; Maazinejad, B.; Ali, V.; Tyagi, I.; Gupta, V.K.: Enhanced removal of toxic Congo red dye using multi walled carbon nanotubes: kinetic, equilibrium studies and its comparison with other adsorbents. J. Mol. Liq. **212**, 266–271 (2015)
4. Husain, Q.; Ulber, R.: Immobilized peroxidase as a valuable tool in the remediation of aromatic pollutants and xenobiotic compounds: a review. Crit. Rev. Environ. Sci. Technol. **41**, 770–804 (2011)
5. Cano, O.A.; González, C.R.; Paz, J.H.; Madrid, P.A.; Casillas, P.G.; Hernández, A.M.; Pérez, C.M.: Catalytic activity of palladium nanocubes/multiwalled carbon nanotubes structures for methyl orange dye removal. Catal. Today **282**, 168–173 (2017)
6. Rubangakene, N.O.; Elkady, M.; Elwardany, A.; Fujii, M.; Sekiguchi, H.; Shokry, H.: Effective decontamination of methylene blue from aqueous solutions using novel nano-magnetic biochar from green pea peels. Environ. Res. **220**, 115272 (2023)
7. Faryadi, M.; Rahimi, M.; Akbari, M.: Process modeling and optimization of Rhodamine B dye ozonation in a novel microreactor equipped with high frequency ultrasound wave. Korean J. Chem. Eng. **33**, 922–933 (2016)
8. Robinson, P.K.: Enzymes: principles and biotechnological applications. Essays Biochem. **59**, 75 (2015)
9. Mohan, S.V.; Prasad, K.K.; Rao, N.C.; Sarma, P.N.: Acid azo dye degradation by free and immobilized horseradish peroxidase (HRP) catalyzed process. Chemosphere **58**, 1097–1105 (2005)
10. Bilal, M.; Asgher, M.; Iqbal, H.M.; Hu, H.; Zhang, X.: Bio-based degradation of emerging endocrine-disrupting and dye-based pollutants using cross-linked enzyme aggregates. Environ. Sci. Pollut. Res. **24**, 7035–7041 (2017)
11. Lai, Y.C.; Lin, S.C.: Application of immobilized horseradish peroxidase for the removal of p-chlorophenol from aqueous solution. Process Biochem. **40**, 1167–1174 (2005)
12. Altikatoglu, Y.M.; Attar, A.: An accomplished procedure of horseradish peroxidase immobilization for removal of Acid yellow 11 in aqueous solutions. Water Sci. Technol. **81**, 2664–2673 (2020)
13. Jankowska, K.; Zdarta, J.; Grzywaczyk, A.; Degórska, O.; Kijeńska-Gawrońska, E.; Pinelo, M.; Jesionowski, T.: Horseradish peroxidase immobilised onto electrospun fibres and its application in decolourisation of dyes from model sea water. Process Biochem. **102**, 10–21 (2021)
14. Wang, Y.J.; Xu, K.Z.; Ma, H.; Liao, X.R.; Guo, G.; Tian, F.; Guan, Z.B.: Recombinant horseradish peroxidase C1A immobilized on hydrogel matrix for dye decolorization and its mechanism on Acid blue 129 decolorization. Appl. Biochem. Biotechnol. **192**, 861–880 (2020)
15. Henriksen, A.A.; Smith, T.; Gajhede, M.: The structures of the horseradish peroxidase C-ferulic acid complex and the ternary complex with cyanide suggest how peroxidases oxidize small phenolic substrates. J. Biol. Chem. **274**, 35005–35011 (1999)
16. Newmyer, S.L.; Ortiz de Montellano, P.R.: Horseradish peroxidase His42Ala, His42Val, and Phe41Ala mutants: histidine catalysis and control of substrate access to the heme iron. J. Biol. Chem. **270**, 19430–19438 (1995)
17. Rodriguez-Lopez, J.N.; Smith, A.T.; Thorneley, R.N.F.: Role of arginine 38 in horseradish peroxidase: a critical residue for substrate binding and catalysis. J. Biol. Chem. **271**, 4023–4030 (1996)
18. Gajhede, M.; Schuller, D.J.; Henriksen, A.; Smith, A.T.; Poulos, T.L.: Crystal structure of horseradish peroxidase C at 2.15 angstrom resolution. Nat. Struct. Biol. **4**, 1032–1038 (1997)
19. Henriksen, A.; Schuller, D.J.; Meno, K.; Welinder, K.G.; Smith, A.T.; Gajhede, M.: Structural interactions between horseradish peroxidase C and the substrate benzhydroxamic acid determined by X-ray crystallography. Biochemistry **37**, 8054–8060 (1998)
20. Ator, M.; Ortiz de Montellano, P.R.: Protein control of prosthetic heme reactivity. Reaction of substrates with the heme edge of horseradish peroxidase. J. Biol. Chem. **262**, 1542–1551 (1987)
21. Ugarova, N.N.; Kutuzova, G.D.; Rogozhin, V.V.; Berezin, I.V.: Functionally important carboxyl groups of horseradish peroxidase. Biochim. Biophys. Acta Protein Struct. Mol. Enzymol. **790**(1), 22–30 (1984)
22. Gholami-Borujeni, F.; Mahvi, A.H.; Naseri, S.; Faramarzi, M.A.; Nabizadeh, R.; Alimohammadi, M.: Application of immobilized horseradish peroxidase for removal and detoxification of azo dye from aqueous solution. Res. J. Chem. Environ **15**, 217–222 (2011)
23. Keshta, B.E.; Gemea, A.H.; Khamis, A.A.: Impacts of horseradish peroxidase immobilization onto functionalized superparamagnetic

iron oxide nanoparticles as a biocatalyst for dye degradation. Environ. Sci. Pollut. Res. **29**, 6633–6645 (2022)
24. Bilal, M.; Adeel, M.; Rasheed, T.; Zhao, Y.; Iqbal, H.M.: Emerging contaminants of high concern and their enzyme-assisted biodegradation–a review. Environ. Int. **124**, 336–353 (2019)
25. Garcia-Galan, C.; Berenguer-Murcia, Á.; Fernandez-Lafuente, R.; Rodrigues, R.C.: Potential of different enzyme immobilization strategies to improve enzyme performance. Adv. Synth. Catal. **353**, 2885–2904 (2011)
26. Imam, H.T.; Marr, P.C.; Marr, A.C.: Enzyme entrapment, biocatalyst immobilization without covalent attachment. Green Chem. **23**, 4980–5005 (2021)
27. Sheldon, R.A.: Enzyme immobilization: the quest for optimum performance. Adv. Synth. Catal. **349**, 1289–1307 (2007)
28. Vineh, M.B.; Saboury, A.A.; Poostchi, A.A.; Rashidi, A.M.; Parivar, K.: Stability and activity improvement of horseradish peroxidase by covalent immobilization on functionalized reduced graphene oxide and biodegradation of high phenol concentration. Int. J. Biol. Macromol. **106**, 1314–1322 (2018)
29. Ozer, E.T.; Osman, B.; Kara, A.; Demirbel, E.; Besirli, N.; Gucer, S.: Diethyl phthalate removal from aqueous phase using poly(EGDMA-MATrp) beads: kinetic, isothermal and thermodynamic studies. Environ. Technol. **36**, 1698–1706 (2015)
30. Altikatoglu, M.; Arioz, C.; Basaran, Y.; Kuzu, H.: Stabilization of horseradish peroxidase by covalent conjugation with dextran aldehyde against temperature and pH changes. Open Chem. **7**, 423–428 (2009)
31. Tavares, T.S.; da Rocha, E.P.; Esteves Nogueira, F.G.; Torres, J.A.; Silva, M.C.; Kuca, K.; Ramalho, T.C.: Δ-FeOOH as support for immobilization peroxidase: optimization via a chemometric approach. Molecules **25**, 259 (2020)
32. Hermanová, S.; Zarevúcká, M.; Bouša, D.; Pumera, M.; Sofer, Z.: Graphene oxide immobilized enzymes show high thermal and solvent stability. Nanoscale **7**, 5852–5858 (2015)
33. Bindu, V.U.; Shanty, A.A.; Mohanan, P.V.: Parameters affecting the improvement of properties and stabilities of immobilized α-amylase on chitosan-metal oxide composites. Int. J. Biochem. Biophys. **6**, 44–57 (2018)
34. Sun, H.; Jin, X.; Long, N.; Zhang, R.: Improved biodegradation of synthetic azo dye by horseradish peroxidase cross-linked on nanocomposite support. Int. J. Biol. Macromol. **95**, 1049–1055 (2017)
35. Jiang, Y.; Tang, W.; Gao, J.; Zhou, L.; He, Y.: Immobilization of horseradish peroxidase in phospholipid-templated titania and its applications in phenolic compounds and dye removal. Enzyme Microb. Technol. **55**, 1–6 (2014)
36. Pan, C.; Ding, R.; Dong, L.; Wang, J.; Hu, Y.: Horseradish peroxidase-carrying electrospun nonwoven fabrics for the treatment of o-methoxyphenol. J. Nanomater. **2015**, 616879 (2015)
37. Wajs, E.; Caldera, F.; Trotta, F.; Fragoso, A.: Peroxidase-encapsulated cyclodextrin nanosponge immunoconjugates as a signal enhancement tool in optical and electrochemical assays. Analyst **139**, 375–380 (2014)
38. Šekuljica, N.Ž; Prlainović, N.Ž; Jovanović, J.R.; Stefanović, A.B.; Djokić, V.R.; Mijin, D.Ž; Knežević-Jugović, Z.D.: Immobilization of horseradish peroxidase onto kaolin. Bioprocess Biosyst. Eng. **39**, 461–472 (2016)
39. Mohamed, S.A.; Darwish, A.A.; El-Shishtawy, R.M.: Immobilization of horseradish peroxidase on activated wool. Process Biochem. **48**, 649–655 (2013)
40. Mohamed, S.A.; Al-Harbi, M.H.; Almulaiky, Y.Q.; Ibrahim, I.H.; El-Shishtawy, R.M.: Immobilization of horseradish peroxidase on Fe_3O_4 magnetic nanoparticles. Electron. J. Biotechnol. **27**, 84–90 (2017)
41. Temoçin, Z.; Yiğitoğlu, M.: Studies on the activity and stability of immobilized horseradish peroxidase on poly (ethylene terephthalate) grafted acrylamide fiber. Bioprocess Biosyst. Eng. **32**, 467–474 (2009)
42. Li, N.; Yin, H.; Pei, J.; Huang, Y.; Xu, G.; Yuan, H.; Yang, Y.: A novel ship-in-bottle type immobilized HRP via co-adsorption of super paramagnets and HRP into silica hollow fiber. J. Inorg. Organomet. Polym. Mater. **28**, 751–766 (2018)
43. Noma, S.A.A.; Ulu, A.; Acet, Ö.; Sanz, R.; Sanz-Pérez, E.S.; Odabaşı, M.; Ateş, B.: Comparative study of ASNase immobilization on tannic acid-modified magnetic Fe_3O_4/SBA-15 nanoparticles to enhance stability and reusability. New J. Chem. **44**, 4440–4451 (2020)
44. Almulaiky, Y.Q.; El-Shishtawy, R.M.; Aldhahri, M.; Mohamed, S.A.; Afifi, M.; Abdulaal, W.H.; Mahyoub, J.A.: Amidrazone modified acrylic fabric activated with cyanuric chloride: a novel and efficient support for horseradish peroxidase immobilization and phenol removal. Int. J. Biol. Macromol. **140**, 949–958 (2019)
45. Singer, S.J.: The properties of proteins in nonaqueous solvents. Adv. Protein Chem. **17**, 1–68 (1962)
46. Lee, S.B.; Kim, K.J.: Effect of water activity on enzyme hydration and enzyme reaction rate in organic solvents. J. Ferment. Bioeng. **79**, 473–478 (1995)
47. Nakajima, H.; Suzuki, K.; Imahori, K.: Effects of various organic solvents on the activity of thermolysin. Agric. Biol. Chem. **49**, 317–323 (1975)
48. Lopes, L.A.; Dias, L.P.; da Costa, H.P.S.; da Silva Neto, J.X.; Morais, E.G.; de Oliveira, J.T.A.; de Sousa, D.D.O.B.: Immobilization of a peroxidase from Moringa oleifera Lam. roots (MoPOX) on chitosan beads enhanced the decolorization of textile dyes. Process Biochem. **110**, 29–141 (2021)
49. Alshawafi, W.M.; Aldhahri, M.; Almulaiky, Y.Q.; Salah, N.; Moselhy, S.S.; Ibrahim, I.H.; Mohamed, S.A.: Immobilization of horseradish peroxidase on PMMA nanofibers incorporated with nanodiamond. Artif. Cells Nanomed. Biotechnol. **46**, 973–981 (2018)
50. Ulu, A.; Noma, S.A.A.; Koytepe, S.; Ates, B.: Magnetic Fe_3O_4@MCM-41 core–shell nanoparticles functionalized with thiol silane for efficient L-asparaginase immobilization. Artif. Cells Nanomed. Biotechnol. **46**, 1035–1045 (2018)
51. Bayramoglu, G.; Altintas, B.; Yakup Arica, M.: Cross-linking of horseradish peroxidase adsorbed on polycationic films: utilization for direct dye degradation. Bioprocess Biosyst. Eng. **35**, 1355–1365 (2012)
52. Samui, A.; Sahu, S.K.: One-pot synthesis of microporous nanoscale metal organic frameworks conjugated with laccase as a promising biocatalyst. New J. Chem. **42**, 4192–4200 (2018)
53. Ahmed, S.A.; Abdella, M.A.A.; El-Sherbiny, G.M.: Catalytic, kinetic and thermal properties of free and immobilized Bacillus subtilis-MK1 α-amylase on Chitosan-magnetic nanoparticles. Biotechnol. Rep. **26**, e00443 (2020)
54. Aravindhan, R.; Rao, J.R.; Nair, B.U.: Removal of basic yellow dye from aqueous solution by sorption on green alga Caulerpa scalpelliformis. J. Hazard. Mater. **142**, 68–76 (2007)
55. Aksu, Z.; Karabayır, G.: Comparison of biosorption properties of different kinds of fungi for the removal of Gryfalan Black RL metal-complex dye. Bioresour. Technol. **99**, 7730–7741 (2008)
56. Kasai, T.; Wada, T.; Iijima, T.; Minami, Y.; Sakaguchi, T.; Koga, R.; Shiratori, T.; Otsuka, Y.; Shimada, Y.; Okayama, Y.; Goto, S.: Comparative study of the hydrophobic interaction effect of pH and ionic strength on aggregation/emulsification of Congo red and amyloid fibrillation of insulin. BBA Adv. **2**, 100036 (2022)
57. Cardoso, N.F.; Pinto, R.B.; Lima, E.C.; Calvete, T.; Amavisca, C.V.; Royer, B.; Cunha, M.L.; Fernandes, T.H.M.; Pinto, I.S.: Removal of remazol black B textile dye from aqueous solution by adsorption. Desalination **269**, 92–103 (2011)

58. Li, Z.; Qiu, C.; Gao, J.; Wang, H.; Qin, M.: Improving lignin removal from pre-hydrolysis liquor by horseradish peroxidase-catalyzed polymerization. Sep. Purif. Technol. **212**, 273–279 (2019)
59. Kurtuldu, A.; Eşgin, H.; Yetim, N.K.; Semerci, F.: Immobilization horseradish peroxidase onto UiO-66-NH_2 for biodegradation of organic dyes. J. Inorg. Organomet. Polym. Mater. **32**, 2901–2909 (2022)
60. Farias, S.; Mayer, D.A.; de Oliveira, D.; de Souza, S.; de Souza, A.A.U.: Free and Ca-alginate beads immobilized horseradish peroxidase for the removal of reactive dyes: an experimental and modeling study. Appl. Biochem. Biotechnol. **182**, 1290–1306 (2017)
61. Li, X.; Wu, Z.; Tao, X.; Li, R.; Tian, D.; Liu, X.: Gentle one-step co-precipitation to synthesize bimetallic CoCu-MOF immobilized laccase for boosting enzyme stability and Congo red removal. J. Hazard. Mater. **438**, 129525 (2022)
62. Bilal, M.; Iqbal, H.M.; Hu, H.; Wang, W.; Zhang, X.: Enhanced biocatalytic performance and dye degradation potential of chitosan-encapsulated horseradish peroxidase in a packed bed reactor system. Sci. Total. Environ. **575**, 1352–1360 (2017)
63. Banotra, D.; Sharma, S.; Khandegar, V.: Application of modified Fe_3O_4 nanocomposites for dye removal: equilibrium, kinetic, and thermodyanmic study. J. Hazard Toxic Radioact. Waste **26**, 06021004 (2022)
64. Borza, P.; Benea, I.C.; Bitcan, I.; Todea, A.; Muntean, S.G.; Peter, F.: Enzymatic degradation of azo dyes using peroxidase immobilized onto commercial carriers with epoxy groups. Stud. Univ. Babes-Bolyai, Chem. **65**, 279–290 (2020)